

# solar Air Heaters

This chapter deals with the description and analysis of various types of solar air heaters. The principal applications in which solar air heaters are used are drying for agricultural and industrial purposes, and space heating. Indeed, they are the logical choice for these applications, compared to liquid flat-plate collectors, because they eliminate the need to transfer heat from one fluid to another.

## 5.1 INTRODUCTION

A conventional solar air heater generally consists of an absorber plate with a parallel plate below forming a passage of high aspect ratio through which the air to be heated flows. As in the case of the liquid flat-plate collector, a transparent cover system is provided above the absorber plate, while a sheet metal container filled with insulation is provided on the bottom and sides. The arrangement is sketched in Fig. 5.1 (a). Two other arrangements, which are not so common, are also shown in Fig. 5.1. In the arrangement shown in Fig. 5.1 (b), the air to be heated flows between the cover and the absorber plate itself instead of through a separate passage, while in Fig. 5.1 (c), the air flows between the cover and the absorber plate, as well as through the passage below the absorber plate.

Like a liquid flat-plate collector, a solar air heater is simple in design

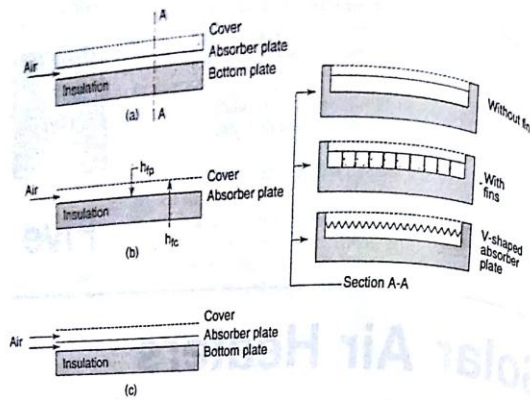


Fig. 5.1 Various Types of Solar Air Heaters

freeze, the solar air heater has the advantage of not requiring any special attention at temperatures below  $0^{\circ}\text{C}$ . Corrosion and leakage problems are also less severe. However, the value of the heat transfer coefficient between the absorber plate and the air is low and this results in a lower efficiency. For this reason, the surfaces are sometimes roughened or longitudinal fins are provided in the air-flow passage. Another variation is to use a V-shaped or corrugated absorber plate [see Sec. A-A, Fig. 5.1 (a)].

A further disadvantage associated with the use of a solar air heater is that large volumes of fluid have to be handled. As a result, the electrical power required to blow the air through a system can be significant if the pressure drop is not kept within prescribed limits.

The face areas of solar air heaters range from 1 to  $2\text{ m}^2$ . Materials of construction and sizes are similar to those used with liquid flat-plate collectors (see Sec. 4.1). Thus, the absorber plate is a metal sheet about 1 mm in thickness, usually made of GI or steel. Glass of thickness 4 to 5 mm is the most commonly used cover material. However, plastics are being used in increasing numbers. Mineral wool or glass wool of thickness 5 to 8 cm is used for the bottom and side insulation. The whole assembly is contained in a sheet metal box and inclined at a suitable angle.

Compared to liquid flat-plate collectors, the pace of commercialisation for the production of solar air heaters has been slow all over the world. This is true in India as well, where they have been used primarily in systems for forced convection drying of various kinds of agricultural products. Only about 100 such systems have been installed

so far. The reason for the slow pace is the fact that drying of agricultural products is a seasonal activity, requiring energy for only a few months. As a result, the drying systems remain idle for a large part of the year and the economics in terms of the payback period is poor. It seems essential to pursue other applications like drying for industrial purposes and space heating in the northern parts of the country if the market for solar air heaters is to increase.

## 5.2 PERFORMANCE ANALYSIS OF A CONVENTIONAL AIR HEATER

We now consider the performance analysis of the conventional air heater shown in Fig. 5.1 (a). The heater has an absorber plate of length  $L_1$  and width  $L_2$ . The air flows in a parallel plate passage below the absorber plate. Details are shown in Fig. 5.2.

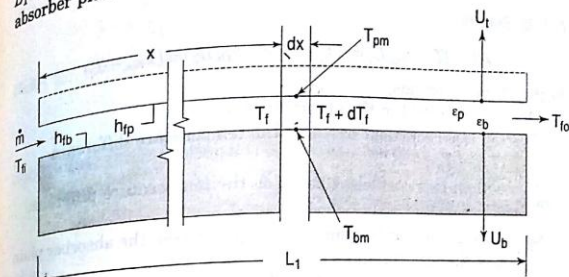


Fig. 5.2 Analysis of a Conventional Solar Air Heater

The analysis is due to Whillier\* and proceeds along lines identical to those adopted for the liquid flat-plate collector (Chapter 4) for the calculation of  $(\tau\alpha)_b$ ,  $(\tau\alpha)_d$ ,  $U_t$  and  $U_b$ . Considering a slice of width  $L_2$  and thickness  $dx$  at a distance  $x$  from the inlet, we write down energy balances for the absorber plate, the plate below it, and the air flowing in between. We assume that (i) the bulk mean temperature of the air changes from  $T_f$  to  $(T_f + dT_f)$  as it flows through the distance  $dx$ , (ii) the air mass flow rate is  $\dot{m}$ , (iii) the mean temperatures of the absorber plate and the plate below are  $T_{pm}$  and  $T_{bm}$  respectively and their

\*A. Whillier, "Black-painted Solar Air Heaters of Conventional Design", *Solar Energy*, 8, 31 (1963).

### Conventional Air Heater with Continuous Longitudinal Fins

The addition of continuous longitudinal fins to the bottom side of the absorber plate improves the heat transfer. This is desirable because it increases the efficiency. We now analyse such a heater in which fins of height  $L_f$  and thickness  $\delta_f$  are spaced at a distance  $W$  centre-to-centre apart (Fig. 5.3). The distance between the absorber plate and the bottom plate is  $L$ . Consequently the clearance between the fins and the bottom plate is  $(L - L_f)$ . Considering a slice of width  $W$  and thickness  $dx$  at a distance  $x$  from the inlet, we again write down energy balances for the absorber plate, the bottom plate, and the air flowing in between. The assumptions made earlier in Sec. 5.2 are again made. We get

$$S W dx = U_t W dx (T_{pm} - T_a) + h_{fp} W dx (T_{pm} - T_f) + 2L_f dx \phi_f h_{ff} (T_{pm} - T_f) + h_r W dx (T_{pm} - T_{bm}) \quad (5.34)$$

$$h_r W dx (T_{pm} - T_{bm}) = h_{fb} W dx (T_{bm} - T_f) + U_b W dx (T_{bm} - T_a) \quad (5.35)$$



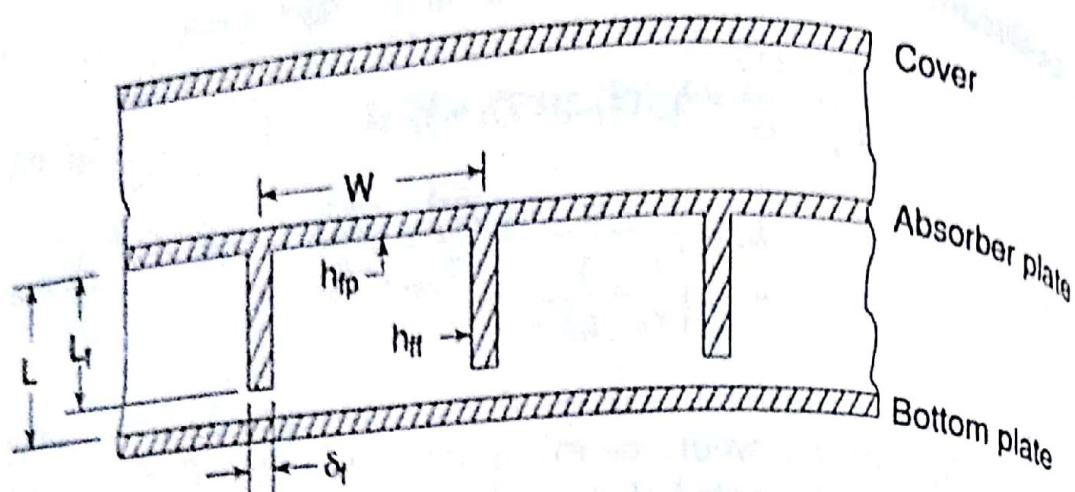


Fig. 5.3 Conventional Air Heater with Fins

$$\frac{W}{L_2} \dot{m} C_p dT_f = h_{fp} W dx (T_{pm} - T_f) + 2L_f dx \phi_f h_{ff} (T_{pm} - T_f) + h_{fb} W dx (T_{bm} - T_f) \quad (5.36)$$

It will be seen that additional terms are introduced in Eqs (5.34) and (5.36) to take account of heat transfer from the fin surfaces.

In these equations,

$\phi_f$  = fin effectiveness,\*

$h_{ff}$  = convective heat transfer coefficient between the fin surface and the air stream,

$h_r$  = equivalent radiative heat transfer coefficient†

As in Sec. 5.2, we delete the bottom loss term from Eq. (5.35) and club it with the top loss term in Eq. (5.34). Eqs (5.34) to (5.36) then simplify to

$$S = U_i (T_{pm} - T_a) + h_{fp} \left( 1 + \frac{2L_f \phi_f h_{ff}}{W h_{fp}} \right) (T_{pm} - T_f) + h_r (T_{pm} - T_{bm}) \quad (5.37)$$

$$h_r (T_{pm} - T_{bm}) = h_{fb} (T_{bm} - T_f) \quad (5.38)$$

$$\frac{\dot{m} C_p}{L_2} \frac{dT_f}{dx} = h_{fp} \left( 1 + \frac{2L_f \phi_f h_{ff}}{W h_{fp}} \right) (T_{pm} - T_f) + h_{fb} (T_{bm} - T_f) \quad (5.39)$$

Equations (5.37) to (5.39) become the same as Eqs (5.5) to (5.7) if

$h_{fp} \left( 1 + \frac{2L_f \phi_f h_{ff}}{W h_{fp}} \right)$  is replaced by  $h_{fp}$ . Thus, the solutions given in

$$f = 0.06006 \times 3635^{-0.2352} = 0.008734$$

Therefore

$$\text{Pressure drop} = \frac{4 \times 0.008734 \times 1.060 \times 2 \times 3.900^2}{2 \times 0.01768}$$

$$= 31.85 \text{ N/m}^2$$

Comparing these results with those of Example 5.1, we see that the efficiency of the air heater has increased significantly from 42.5 per cent to 49.8 per cent, a gain of 7.3 per cent in absolute terms. However, the pressure drop has also increased by a factor of 2 from  $15.78 \text{ N/m}^2$  to  $31.85 \text{ N/m}^2$ .

Some experimental studies\* on finned solar air heaters are available. These also indicate a substantial improvement in efficiency. However, as seen in Example 5.2, the addition of fins introduces an extra pressure drop. Thus, there is an optimum spacing below which it does not pay to increase the number of fins because of the increased pressure drop.

#### Two-pass Solar Air Heater

Satcunanathan and Deonarinet have suggested the use of a two-pass solar air heater in order to reduce the losses from the top. They constructed a unit in which the air was first passed between the covers of a two-glass cover heater and then under the absorber plate (Fig. 5.4 (a)). When operated as an open system with inlet air at ambient temperature, it was found that the outer glass cover temperature was lowered by 2 to 5°C and that it operated nearer the ambient temperature. As a result, the losses were reduced and the efficiency of the collector was measured to be 10 to 15 per cent higher than of a conventional heater.

Subsequently Wijeyesundera *et al.*† have studied the two-pass concept in greater detail both analytically and experimentally. Two two-pass flow arrangements were considered. One arrangement was the same as the one studied by Satcunanathan and Deonarinet (Fig. 5.4 (a)), while in the other, the inlet air flowed first above the absorber plate and then under it (Fig. 5.4 (b)). For open systems, with inlet air at ambient temperature, both the two-pass arrangements gave an efficiency of about 10–15 per cent more than the conventional single pass arrange-

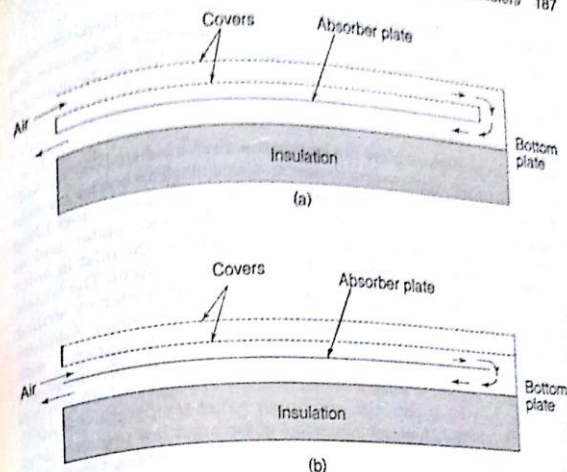


Fig. 5.4 Two-pass Solar Air Heater

ment over a wide range of operating conditions. However, for closed air recirculating systems, the two-pass arrangements yielded a better performance only up to a certain value of the difference between the air inlet temperature to the collector and the ambient temperature. With the arrangement shown in Fig. 5.4 (a), the two-pass design was found to be better than the single pass design up to an inlet air temperature difference of 20°C, while with the arrangement shown in Fig. 5.4 (b), the two-pass design was better up to an inlet air temperature difference of 50°C.

#### 5.3.2 Some Novel Designs

A number of novel designs have also been suggested from time to time by many investigators. Some of these will now be briefly described. They are (i) the overlapped glass plate air heater, (ii) the matrix air heater, (iii) the honeycomb porous-bed air heater, (iv) the all-plastic air heater, and (v) the jet plate air heater. In the first four designs, the air flows through the absorbing surface. For this reason, they are referred to as collectors with porous absorbers. Such collectors generally yield higher efficiencies than conventional designs. In addition, because of larger flow areas, they have smaller pressure drops. In spite of these advantages, they have not been used extensively. A possible deterrent could be the fact that the air flows directly under the cover.

\*T.M. Kuzay, M.A.S. Malik and K.W. Boer, "Solar Collectors of Solar One", *Proc. Workshop Solar Collectors Heating Cooling Buildings*, 99 (1974).

†S. Satcunanathan and S. Deonarinet, "A Two-pass Solar Air Heater", *Solar Energy*, 15, 41 (1973).

‡N.E. Wijeyesundera, L.L. Ah and L.E. Tjioe, "Thermal Performance Study of Two-pass Solar Air Heaters", *Solar Energy*, 28, 363 (1982).



### Honeycomb Porous-bed Air Heater

The honeycomb porous-bed air heater was suggested by Lalude and Buchberg.\* It is a variation on the matrix air heater, a honeycomb being placed over the matrix (Fig. 5.7). Because of the presence of the honeycomb, the top losses are reduced. Measurements made with a test module having a rectangular honeycomb yielded very high collection efficiencies, between 78 and 67 per cent, corresponding to values of  $(\bar{T}_f - T_a)/I_T$  equal to 18 and 53 °C-m<sup>2</sup>/kW. The honeycomb used was selectively reflecting, the ratio of the depth of the honeycomb to the smaller side of the rectangle was 7.1, while that of the two sides of the rectangle was 3.4.

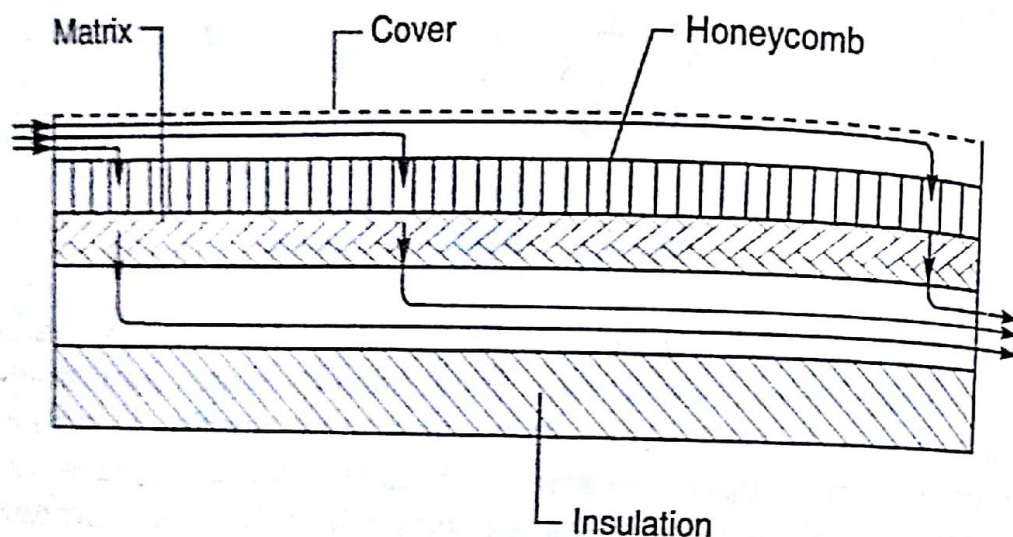


Fig. 5.7 Honeycomb Porous-bed Air Heater

All-plastic Air Heater

significant improvement in the useful heat gain and the collection efficiency. For the specific case of a spacing of 10 cm between the absorber plate and the bottom plate and a flow length of 2 m, the increase in efficiency was calculated to be 26.5 per cent for a mass flow rate per unit area of  $50 \text{ kg/h-m}^2$ . However, the authors have not calculated the additional pressure drop associated with the introduction of the jet plate. This is also likely to be significant.

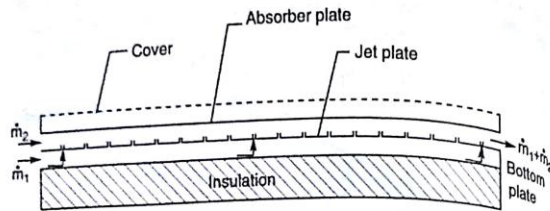


Fig. 5.9 Jet Plate Solar Air Heater

#### 5.4 TESTING PROCEDURES

The standard procedures suggested for testing solar air heaters are similar in most respects to those described in Sec. 4.12 for testing liquid flat-plate collectors. A schematic diagram showing the essential features of the test set-up is shown in Fig. 5.10. It is a closed loop consisting of the solar air heater to be tested, a blower and an apparatus for reconditioning the air which ensures that the air enters the air heater at the desired temperature  $T_{fi}$ . Provision is made for measuring the same quantities specified earlier. Some precautions are, however, necessary. Since the fluid is air, it has to be ensured that it is well mixed at the exit from the air heater before its temperature is measured. The mixing is achieved with the help of vanes. As an additional precaution, the temperature both at the inlet and exit of the air heater is measured at a number of locations across the duct cross section.

Measurements are made under the conditions specified earlier and the results are also presented in the same manner. A typical set of results given by Gupta and Garg\* is shown in Fig. 5.11. It will be noted that the European practice of plotting the parameter  $(\bar{T}_f - T_a)/I_T$  on the

\*C.L. Gupta and H.P. Garg, "Performance Studies of Solar Air Heaters", *Solar Energy*, 11, 25 (1967).

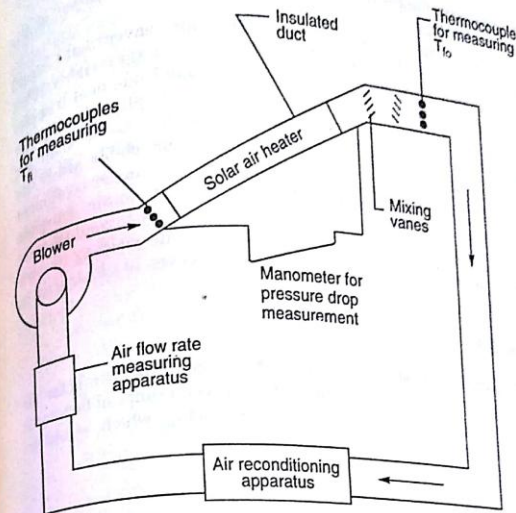
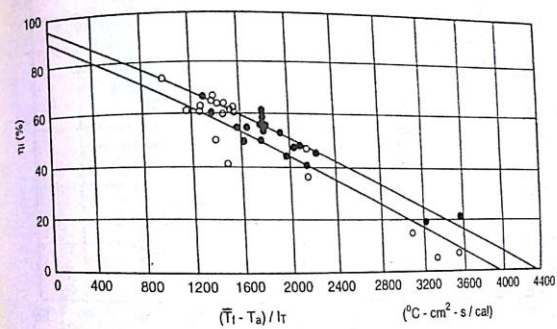


Fig. 5.10 Schematic Diagram of Set-up for Testing Solar Air Heaters

Fig. 5.11 Typical Performance Curves for Two Solar Air Heaters Using  
Gupta and Garg's Data. From Gupta and Garg. Used With

x-axis has been followed. It will also be seen that the scatter of the data is again large.

It has been mentioned in Sec. 4.12 that for conventional liquid flat-plate collectors, changes in the value of  $\dot{m}$  do not appreciably affect the performance because of high values of the liquid side heat transfer coefficient  $h_f$ . A single test curve is, therefore, generally adequate for predicting the behaviour of such collectors. In the case of solar air heaters, however, changes in the values of  $\dot{m}$  appreciably affect the performance because the value of the air side heat transfer coefficient ( $h_{fp}$ ) is relatively low. For this reason, in order to obtain complete information on a solar air heater, it becomes necessary to conduct tests over a range of mass flow rates with each flow rate yielding its own efficiency curve. The use of the performance curves is illustrated in Example 5.3.

#### Example 5.3

The efficiency curves shown in Fig. 5.12 are obtained for a solar air heater ( $L_1 = 1.2$  m,  $L_2 = 0.9$  m) which is tested over a range of flow rates varying from 25 to 200 kg/h. Find the efficiency which would be

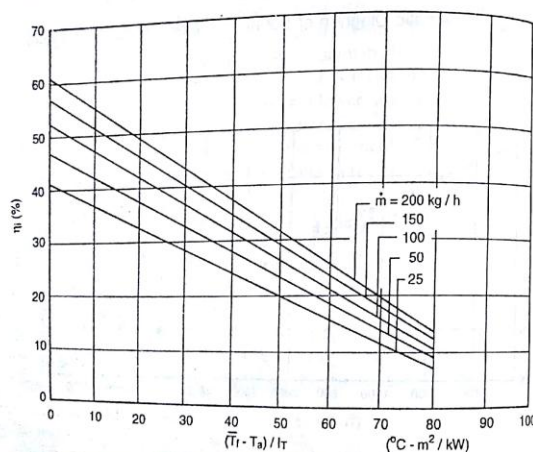


Fig. 5.12 Data for Example 5.2 ( $\eta_i$  is Based on Absorber Plate Area)

obtained and the corresponding mass flow rate if the air heater is used under the following conditions:

Air inlet temperature	= 55°C
Air outlet temperature	= 75°C
Ambient temperature	= 27°C
Solar flux incident on collector face	= 950 W/m <sup>2</sup>

For the given conditions, the x-axis parameter

$$(\bar{T}_f - T_a)/I_T = \left( \frac{55 + 75}{2} - 27 \right) / 0.950$$

$$= 40^\circ\text{C} \cdot \text{m}^2/\text{kW}$$

A trial-and-error procedure will be necessary in order to find the required values of  $\eta_i$  and  $\dot{m}$ .

(i) Assume  $\dot{m} = 25$  kg/h.

From Fig. 5.12, the value of  $\eta_i = 24.2$  per cent.

Therefore, useful heat gain rate  $q_u = 0.242 \times 950 \times 1.2 \times 0.9$

$$= 248.3 \text{ W}$$

$$\dot{m} = \frac{q_u}{C_p(T_{fo} - T_{fi})} = \frac{248.3 \times 3600}{1.007 \times (75 - 55) \times 1000} = 44.4 \text{ kg/h}$$

(ii) Since the value of  $\dot{m}$  calculated from the useful heat gain rate does not match the assumed value, we assume  $\dot{m} = 50$  kg/h. This yields

$$\eta_i = 28.0 \text{ per cent}$$

$$q_u = 287.3 \text{ W}$$

$$\dot{m} = 51.4 \text{ kg/h}$$

and

(iii) Assume  $\dot{m} = 51.4$  kg/h.

This yields

$$\eta_i = 28.09 \text{ per cent}$$

$$q_u = 288.3 \text{ W}$$

$$\dot{m} = 51.5 \text{ kg/h}$$

and

We accept these values as the solution to the problem.

## PROBLEMS

1. The following data is given for a conventional solar air heater with one glass cover:

Length of absorber plate	= 1.90 m
Width of absorber plate	= 0.80 m
Spacing between absorber plate and bottom plate	= 2 cm





## concentrating collectors

In Chapters 4 and 5, we have considered flat-plate collectors for heating liquids and gases to temperatures up to and around  $100^{\circ}\text{C}$ . We now take up the description and analysis of some types of concentrating collectors. These are needed when higher temperatures are required. Typical thermal applications requiring the use of concentrators are medium or high temperature energy conversion cycles and numerous systems for supplying industrial process heat at intermediate temperatures from  $100$  to  $400^{\circ}\text{C}$  or at high temperatures above  $400^{\circ}\text{C}$ .

Brief descriptions of a few concentrating collectors have been given in Sec. 2.1. We begin this chapter by mentioning briefly the characteristics associated with concentrating collectors (Sec. 6.1). After this, various terms are defined and typical collector geometries described. Flat-plate collectors with reflectors are considered in Sec. 6.2, and the cylindrical parabolic collector in Sec. 6.3. The tracking modes adopted with it are listed and compared, and a performance analysis of the collector is given. The compound parabolic collector is analysed in Sec. 6.4. The chapter concludes with descriptions of the paraboloidal dish collector in Sec. 6.5 and the central receiver collector in Sec. 6.6.



## 6.1 INTRODUCTION

### 6.1.1 General Characteristics

Concentration of solar radiation is achieved by using a reflecting arrangement of mirrors or a refracting arrangement of lenses. The optical system directs the solar radiation onto an absorber of smaller area which is usually surrounded by a transparent cover. Because of the optical system, certain losses (in addition to those which occur while the radiation is transmitted through the cover) are introduced. These include reflection or absorption losses in the mirrors or lenses, and losses due to geometrical imperfections in the optical system. The combined effect of all such losses is indicated through the introduction of a term called the *optical efficiency*. The introduction of more optical losses is compensated for by the fact that the flux incident on the absorber surface is concentrated on a smaller area. As a result, the thermal loss terms do not dominate to the same extent as in a flat-plate collector and the collection efficiency is usually higher.

It has been noted earlier that some of the attractive features of a flat-plate collector are simplicity of design and ease of maintenance. The same cannot be said of a concentrating collector. Because of the presence of an optical system, a concentrating collector usually has to follow or "track" the sun so that the beam radiation is directed onto the absorber surface. The method of tracking adopted and the precision with which it has to be done varies considerably. In collectors giving a low degree of concentration, it is often adequate to make one or two adjustments of the collector orientation every day. These can be made manually. On the other hand, with collectors giving a high degree of concentration, it is necessary to make continuous adjustments of the collector orientation. The need for some form of tracking introduces a certain amount of complexity in the design. Maintenance requirements are also increased. All these factors add to the cost. An added disadvantage is the fact that much of the diffuse radiation is lost because it does not get focussed.

In the last few years, significant advances have been made in the development of concentrating collectors and a number of types have been commercialised abroad. Almost all of them are line-focussing cylindrical parabolic collectors, and yield temperatures up to 400°C.

### 6.1.2 Definitions

In order to be consistent in the use of terms, we will use the phrase "concentrating collector" to denote the whole system. The term "concentrator" will be used only for the optical subsystem which directs the solar radiation onto the absorber, while the term "receiver" will

normally be used to denote the subsystem consisting of the absorber, its cover and other accessories. We will now define three terms: aperture, concentration ratio and acceptance angle.

The *aperture* ( $W$ ) is the plane opening of the concentrator through which the solar radiation passes. For a cylindrical or linear concentrator, it is characterized by the width, while for a surface of revolution, it is characterized by the diameter of the opening.

The *concentration ratio* ( $C$ ) is the ratio of the effective area of the aperture to the surface area of the absorber. Values of the concentration ratio vary from unity (which is the limiting case for a flat-plate collector) to a few thousand for a parabolic dish.

The *acceptance angle* ( $2\theta_a$ ) is the angle over which beam radiation may deviate from the normal to the aperture plane and yet reach the absorber. Collectors with large acceptance angles require only occasional adjustments, while collectors with small acceptance angles have to be adjusted continuously.

### 6.1.3 Methods of Classification

Concentrating collectors are of various types and can be classified in many ways. They may be of the reflecting type utilizing mirrors or of the refracting type utilizing Fresnel lenses. The reflecting surfaces used may be parabolic, spherical or flat. They may be continuous or segmented. Classification is also possible from the point of view of the formation of the image, the concentrator being either imaging or nonimaging. Further, the imaging concentrator may focus on a line or at a point.

The concentration ratio is also used as a measure for classifying concentrating collectors. Since this ratio approximately determines the operating temperature, this method of classification is equivalent to classifying the collector by its operating temperature range.

A final possibility is to describe concentrating collectors by the type of tracking adopted. Depending upon the acceptance angle, the tracking may be intermittent (one adjustment daily or every few days) or continuous. Further, the tracking may be required about one axis or two axes.

### 6.1.4 Types of Concentrating Collectors

A number of concentrating collector geometries are shown in Fig. 6.1.

\*The quantity defined here is more precisely referred to as the area or geometric

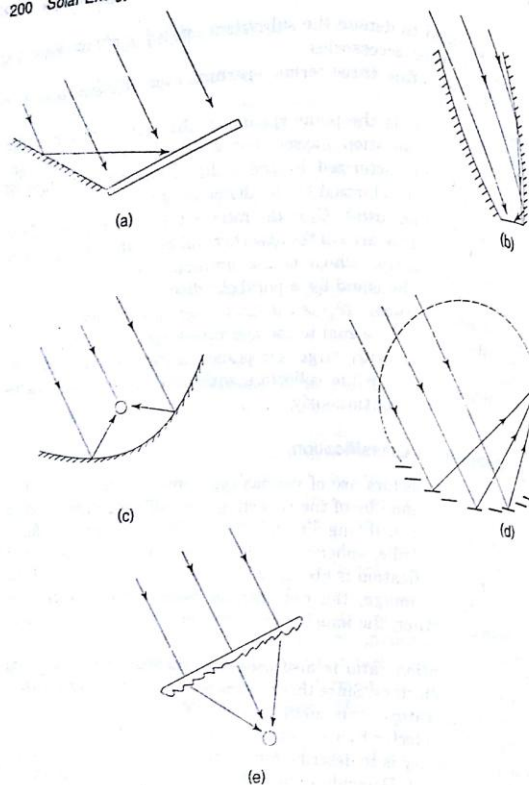


Fig. 6.1 Types of Concentrating Collectors: (a) Flat-plate Collector with Plane Reflectors, (b) Compound Parabolic Collector, (c) Cylindrical Parabolic Collector, (d) Collector with Fixed Circular Concentrator and Moving Receiver, (e) Fresnel Lens Concentrating Collector

The first type shown in Fig. 6.1 (a) is a flat-plate collector with adjustable mirrors at the edges to reflect radiation onto the absorber plate. It is simple in design, has a concentration ratio a little above unity and is useful for giving temperatures about 20 or 30°C higher

than those obtained with a flat-plate collector alone. It is discussed further in Sec. 6.2.

A *compound parabolic collector* (CPC) is shown in Fig. 6.1 (b). The concentrator consists of curved segments which are parts of two parabolas. Like the first type, this collector is also nonimaging. The concentration ratio is moderate and generally ranges from 3 to 10. The main advantage of the compound parabolic collector is that it has a high acceptance angle and consequently requires only occasional tracking. In addition its concentration ratio is equal to the maximum value possible for a given acceptance angle. The CPC is considered in Sec. 6.4.

The next type of collector [Fig. 6.1 (c)] is a *cylindrical parabolic collector* in which the image is formed on the focal axis of the parabola. Many commercial versions of this type are now available. For this reason, it is described and analysed in detail in Sec. 6.3.

Unlike the cylindrical parabolic collector in which the concentrator has to rotate in order to track the sun, the type shown in Fig. 6.1 (d) has a fixed concentrator and a moving receiver. The concentrator is an array of long, narrow, flat mirror strips fixed along a cylindrical surface. The mirror strips produce a narrow line image which follows a circular path as the sun moves. This path is on the same circle on which the mirror strips are fixed. Thus, the receiver has to be moved along the circular path in order to track the sun.

Concentration is also achieved by using lenses. The most commonly used device is the *Fresnel lens* shown in Fig. 6.1 (e). The one shown in the figure is a thin sheet, flat on one side and with fine longitudinal grooves on the other. The angles of these grooves are such that radiation is brought to a line focus. The lens is usually made of extruded acrylic plastic sheets. Line focussing collectors like the ones shown in Figs 6.1 (c), (d), (e) usually have concentration ratios between 10 and 80 and yield temperatures between 150 and 400°C.

In order to achieve higher concentration ratios and temperatures, it becomes necessary to have point focussing rather than line focussing. The point focussing *paraboloid dish collector* has been mentioned earlier in Chapter 2 (Fig. 2.4). Such collectors can have concentration ratios ranging from 100 to a few thousand and have yielded temperatures up to 2000°C. However, from the point of view of the mechanical design, there are limitations to the size of the concentrator and hence, the amount of energy which can be collected by one dish. Commercial versions have been built with dish diameters up to 17 m. In order to collect larger amounts of energy at one point, the *central receiver concept* (see Fig. 2.16) has been adopted. In this case, beam radiation is reflected from a number of independently controlled mirrors called heliostats to a central receiver located at the top of a tower.